2013-12-09

Digital Outcrop Model and Paleoecology of the Eight-Foot Rapid Algal Field (Middle Pennsylvanian Lower Ismay Sequence), Paradox Basin, Utah

Colton Lynn Goodrich
Brigham Young University - Provo

Digital Outcrop Model and Paleoecology of the Eight-Foot Rapid Algal Field (Middle Pennsylvanian Lower Ismay Sequence), Paradox Basin, Utah

Colton Goodrich

A thesis submitted to the faculty of
Brigham Young University
in partial fulfillment of the requirements for the degree of

Master of Science

Scott Ritter, Chair
John McBride
Thomas Morris

Department of Geology

Brigham Young University

December 2013

ABSTRACT

Digital Outcrop Model and Paleoecology of the Eight-Foot Rapid Algal Field (Middle Pennsylvanian Lower Ismay Sequence), Paradox Basin, Utah

Colton Goodrich
Department of Geology, BYU
Master of Science

Although phylloid algal mounds have been studied for 50 year, much remains to be determined concerning the ecology and sedimentology of these Late Paleozoic carbonate buildups. Herein we perform a digital outcrop study of the well-known Middle Pennsylvanian Lower Ismay mound interval in the Paradox Basin because outcropping mounds along the San Juan River are cited as outcrop analogs of reservoir carbonates in the Paradox Basin oil province of Utah and adjacent states. The principal field area is the Eight Foot algal field located at river mile 19.2 on the San Juan River, approximately 14 miles SSW of Bluff, Utah. The Lower Ismay section is exposed on both sides of the river for 1.4 miles. Mechanisms for mound formation are still a heavily debated topic and even now aren't fully understood. While this study does not seek to solely answer this question, it does shed some light on the argument.

A combined total station-LIDAR survey of the exposed Eight Foot mounds indicates that the mound field is comprised of 83 individual and composite mounds that have an average height of 10.9 meters and peak spacing of 48.8 meters. Further, statistical examination of survey data reveals a correlation between mound height and east-west alignment, showing that shelfward mounds were slightly taller than their more basinward counterparts.. However, other shape parameters do not appear to vary systematically across the algal field.

Curve-fitting indicates that the overall mound morphology does not differ significantly from a Gaussian surface indicating that mounds are conical in shape. This suggests that mounds did not form under the influence of directional currents such as waves or tides. Yet, *Ivanovia*-fragment packstone and grainstone facies typical of the mound interval suggest a high-energy depositional setting.

Keywords: Carbonate, algal, 3d, morphology, Ivanovia

ACKNOWLEDGEMENTS

This project, being over two years in the making has had no small amount of help from a melange of people in academics, industry, and in personal associations. In no particular order, I'd like to thank the following.

My parents, Jan and Kevin Goodrich, for all their support in this endeavor.

My mentor and co-author, Dr. Scott Ritter, who for some reason still unknown to me, decided to take a lazy schmuck on as a grad student. Your patience and willingness to help continues to astound me.

Dr. Lisa Stright and Wasiim Benhallam of the University of Utah. Your methodology and advice was invaluable in this endeavor.

Brian Balls, Jon Peterson and Troy Taylor of Summitt Engineering. Your aid in both the canyons of Southern Utah and the hospitality in your home office were most appreciated.

And countless others who made this project possible.

TABLE OF CONTENTS

Contents

INTRODUCTION

Fifty years ago, Pray and Wray (1963) introduced the term "phylloid" algae to distinguish "leaflike" algal remains that occur in Pennsylvanian and Permian carbonate rocks worldwide. Since then, a rich literature on the taxonomy, paleoecology, diagenesis, mineralogy, and sedimentological role of phylloid algae has been published, motivated to a degree by the occurrence of large volumes of oil and gas in "phylloid" algal reservoirs (e.g., Paradox Basin, Utah; Reinecke field, West Texas). These algae are typically associated with mound-shaped, shelf-edge carbonate accumulations in which phylloid algal remains predominate to the near exclusion of other macrobiotic constituents such as corals, bryozoans, brachiopods, and echinoderms. These carbonate accumulations have been variably called phylloid mounds, buildups, banks, bioherms, reefs, and mound complexes. The terminology of these buildups as well as the role of phylloid algae in the construction/accumulation of these positive seafloor features remain as points of discussion (e.g., Ball et al., 1977; Fagerstrom, 1987; Samankassou and West, 2002, 2003; Forsythe, 2003; Grammer and Ritter, 2009.)

Phylloids in algal buildups display a spectrum of growth/preservational forms ranging from *in situ* cones and cups to hydrodynamically accumulated fragments indicating that they performed a range of ecological and sedimentary roles controlled by algal growth form, mode of calcification, and depositional setting. In a few reported occurrences, phylloid algal thalli (small cones or cups) are preserved in growth position and play a direct sedimentary role as frame builders and bafflers in mound construction. For example, phylloid mounds of the Early Permian Laborcita Formation in the Sacramento Mountains with at least 10m of constructional relief contain a predominance of *in situ* phylloids. Cross and Klosterman (1981a) attributed mound development to four complementary process, 1) the growth of erect conical thalli of *Eugonophyllum* (Konishi and Wray, 1961), 2) binding by stromatolites, 3) trapping of carbonate mud (perhaps evidence of interstitial microbial activity), and 4) penecontemporaneous submarine cementation (also see Mazzullo and Cys, 1979). Similar encrustation of erect thalli by cement and encrusting algae was reported from the upper Capitan Limestone (Middle Permian) in the Guadalupe Mountains, west Texas and New Mexico (Babcock, 1977; Toomey and Babcock, 1983). In other instances, phylloid algae with undulatory growth forms such as the red algae *Archaeolithophyllum* form a mass of loosely held undulatory, subhorizontal sheets that baffle sediment and provide sheltered pore spaces (umbrellas or crypts) occupied by microbiota and microbially precipitated peloids (e.g. Samankassou and West, 2002, 2003) thereby forming a locus of sedimentation on the seafloor. These mounds generally have low relief and are laterally persistent (Samankassou and West, 2003).

In most reported occurrences, however, phylloid algal mounds are detrital accumulations of phylloid algal fragments where the paleoecological/sedimentological role of the phylloid algae is unclear because of taphonomic and diagenetic degradation of thalli. Lower Ismay (Pennsylvanian, Desmoinesian) mounds described in the classic paper of Pray and Wray (1963) fall into this category. They described the dominant mound lithology ("sparry algal facies") as "a light-colored, grain-supported porous *Ivanovia* limestone containing abundant sparry calcite" and noted that the "growth habit of this alga cannot be established positively, since only fragmented remains of the leafllike bodies have been observed". With respect to mound development, Pray and Wray (1963, p. 216) envisioned simple accumulation of algal plates below the zone of appreciable wave turbulence in patches on the seafloor where *Ivanovia* grew to the near exclusion of other biota. Recently, Grammer and Ritter (2009) offered a high-energy alternative to Pray and Wray's (1963) parauthochthonous detrital model on the basis of Lower Ismay

outcrops near Eight Foot Rapids in the San Juan River canyon of southeastern Utah. They attributed the fragmental nature of phylloid algal grains and the sinusoidal upper surface of the bioherm interval to the influence of wave- or tide-generated ocean currents, citing dunes and sand waves in *Halimeda*-dominated sand shoals of south Florida as a modern analog.

These outcrop analogs of the productive phylloid mounds of the Aneth field and scores of smaller Paradox Basin oil fields have been described in a number of studies including Brinton (1986), Chidsey et al. (1996), Grammer and Ritter (2009). Additionally, these outcrops have been visited by thousands of geologists and continue to be featured on industry and university field trips. Yet, much remains to be learned about these showcase

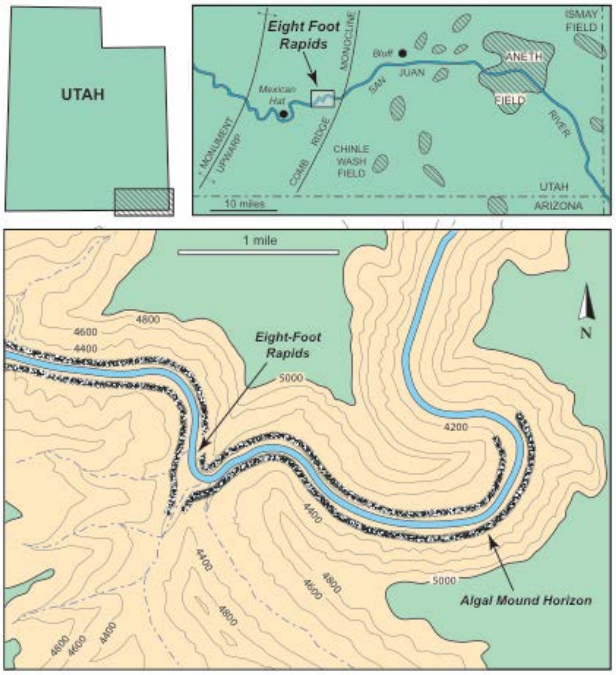

Figure 1. Map showing the location of the Eight-Foot Rapids in southeastern Utah.

phylloid bioherms. The purpose of this study is to comprehensively characterize the morphology, composition, distribution, and reservoir attributes of these mounds and to evaluate the competing low-energy and high-energy models of bioherm development through a joint petrographic and petrophysical analysis tied to a LIDAR-based digital outcrop model of the Lower Ismay bioherm interval. The principal area of interest is the Eight Foot algal field, however, comparative materials are derived from Lower Ismay exposures on the west limb of the Raplee anticline and at Honaker Trail.

Indepth discussion of the mound shapes as they relate to petroleum exploration is another key point. As the algal mounds serve as a primary reservoir for the Aneth field, knowing the morphology of them is important when it comes to extraction. The morphology of the mound shape is ultimately of little note if the mound complexes form an entire interconnected reservoir. However if each mound acts as its own isolated system and there is little communication between reservoirs, knowing the morphology of the mound is integral for maximum extraction of present hydrocarbons.

GEOLOGICAL SETTING

The Paradox Basin is a northwest-southeast trending intracratonic basin that formed in southwestern Colorado and southeastern Utah during the Pennsylvanian Period. During rise of the Uncompahgre uplift of the Ancestral Rockies, the basin subsided rapidly and was filled with over 2000 m of Permo-Pennsylvanian sediments. Stacked depositional sequences accumulated in three roughly parallel facies belts: northeastern clastic wedge (Gianinny and Miskell-Gerhardt, 2009), basin center evaporite belt (Hite, 1969; Rasmussen and Rasmussen, 2009), and southwestern carbonate shelf (Goldhammer et al., 1991). The litho- and chronostratigraphic terminology applied to Pennsylvanian strata in the basin are shown in Figure 2.

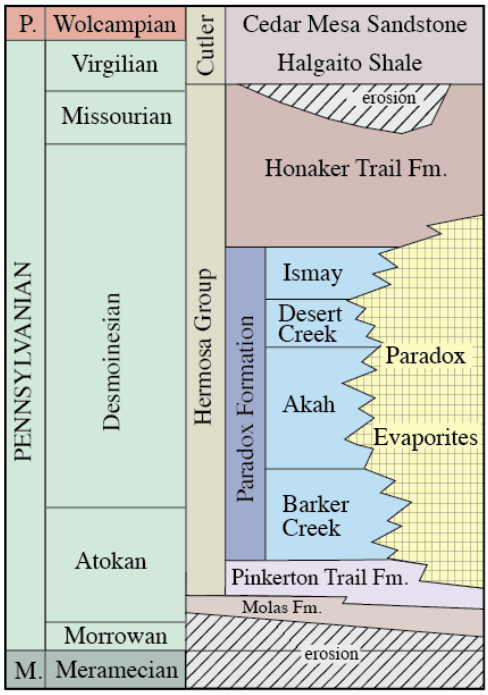

Figure 2. Stratigraphic column showing the Pennsylvanian litho- and chronostratigraphy of the Paradox Basin.

The Paradox Formation is defined as an evaporite facies in the basin center, but includes coeval siliciclastic and carbonate shelf strata. Mixed carbonate-siliclastic strata of the southwestern shelf have been subdivided into six depositional sequences that are, in ascending order, the Barker Creek, Akah, Lower Desert Creek, Upper Desert Creek, Lower Ismay, and Upper Ismay sequences (Golhammer et al., 1991; Gianniny and Simo, 1996). Black "shales" near the base of these sequences correlate with the "C", "A", Chimney Rock, Gothic, and Hovenweep shales of the basin center, respectively (Hite, 1960; Rasmussen and Rasmussen, 2009). The Honaker Trail Formation overlies these sequences and is composed of an upward increase in sandstone and siltstone content reflecting the progressive filling of the Paradox Basin by debris shed from the Uncompahgre uplift.

The Lower Ismay sequence, which is the focus of this paper, is comprised of a single, disconformity-bounded depositional cycle that is characterized by extensive development of phylloid algal mounds observable in both outcrop and in the subsurface (Pray and Wray, 1963; Elias, 1963; Choquette and Traut, 1963; Brinton, 1986). The Lower Ismay is correlated to evaporite cycle 3 of Hite (1960) and evaporite cycle PX3 of Rasmussen and Rasmussen (2009). Conodont data indicate equivalence to the Lower Fort Scott (Excello) cycle of the classic

Midcontinent cyclostratigraphy (Ritter et al., 2002).

METHODS

Collection of Survey Data

Ground-based LIDAR of the Lower Ismay sequence was acquired on both walls of the San Juan River canyon for a distance of 1.9 kilometers (1.2 miles) using a FARO Focus 3D scanner and a set of X survey points. The principal area of study was Eight Foot Rapids, located 14.5 miles west of Bluff, San Juan County, Utah, between river miles 16 and 17 of Willis et al. (1996). A Trimble S6 total station was used to measure control points set beyond the beginning and ending points of the LIDAR scan, as well as at angle points following the river's alignment. This instrument was chosen based on its ability to accurately measure points several hundred feet apart. A Trimble 5800 GPS rover was used to collect static GPS measurements on different control points. This GPS data was post-processed against other known static reference stations to determine geodetic coordinates for the project.

After the river section to be surveyed was determined, a survey prism was set at a primary control point location approximately 50 to 70 meters (150 to 215feet) upstream from the scan position. A second prism was located downstream 400 to 430 meters (1200 to 1300 feet) and positioned so both prisms were visible from scan points in between. A temporary coordinate was used for the first prism location and an assumed bearing was used along with a distance measurement from the station to the second prism to determine its coordinate. These prisms constituted the primary control points for the project.

At every scan position between the two primary control points, the scanner's position was calculated using a resection measurement method. This involved placing the Trimble S6 at the scanner's position and taking measurements to each nearest primary control point. Once the scanner position was calculated, a secondary control target was added and two checkerboard targets were placed approximately 8 to 10 meters (24 to 30 feet) away from the position of the scanner. The center point of the checkerboard was then measured so a coordinate could be calculated at those secondary control point locations. Figure 3 shows the standard range and methodology for the surveys. This process was repeated in a "leap-frog" fashion along the alignment of the river on both sides until the end position was reached. Markers were placed in the ground with a wooded stake at a few of the primary control point locations. The Trimble GPS was set up and GPS data were logged at these locations for post processing.

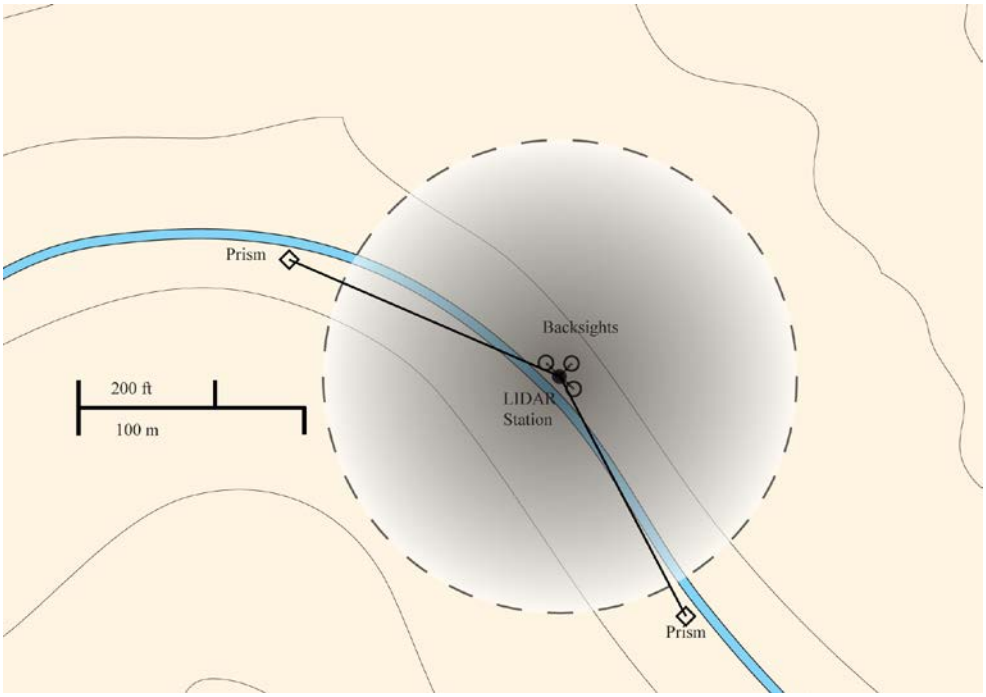

Figure 3. LIDAR station setup along the river. Displayed are the prisms, backsights, and the station itself. The transparent shape represents the data gathered and the falloff related to the range of the machine.

Data Processing

Using the static GPS data logged at various primary control points, true UTM NAD 83 coordinates were determined by uploading data to the National Geodetic Survey's (NGS) Online Positioning User Service (OPUS). OPUS post processed the data collected at the site relative to other GPS base stations in the area and returned corrected positions for the project control points. These corrected positions were used to translate and rotate all primary and secondary control points. The updated coordinates for the secondary control points were used to translate and rotate the LIDAR data produced at each scan location and register it together into one complete whole.

LOWER ISMAY MOUNDS AND ASSOCIATED FACIES

The stratigraphy of the Lower Ismay sequence is shown on Figures 4 and 5. The facies architecture of the sequence has been described by Pray and Wray (1963), Brinton (1986), Goldhammer et al. (1991), Grammer et al. (1996), Grammer et al. (2000), and Grammer and Ritter (2009). Constituent facies are summarized in Table 1. Facies terminology used herein conforms to the terminology established by Pray and Wray (1963) and modified by Goldhammer et al. (1991) and Grammer et al. (1996).

Facies	*Bedding*	*Rock Type*	*Grain Type*	*Depositional Setting*
Quartz Sandstone Facies	Laterally discontinuous sand sheets, trough and ripple cross bedding	Calcaeerous siltstone and fine-grained sandstone, no clay	Quartz, peloids, skeleltal fragments	Marine reworked lowstand eolian sandstone
Black Laminated Mudstone Facies	Laminated	Black sapropelic dolomite, silty	High organic content, quartz silt, clay, dolomite crystals	Maximum flooding, anoxic, low energy environment
Sponge Facies	Laminated, cherty	Mudstone to silty mudstone	Sponge spicules, quartz silt, clay, peloids	Deep subtidal, low oxygen, low energy
Intermediate Facies	Massive bedded, burrowed	Wackestone to packstone	Normal marine skeletal assemblage	Subtidal, well oxygenated, well lit, moderate energy
Mound Base Facies	Massive	Wackestone to packstone	Skeletal grains, peloids, phylloid fragments	Subtidal, well oxygenated, moderate to high energy
Phylloid Algal Facies	Massive to thick bedded, planar cross bedding away from mound center	Packstone to grainstone; bafflestone?	Phylloid algal fragments of genus *Ivanovia*, forams, brachiopods, ostracodes	Shallow subtidal, photic zone, zone of relatively high energy
Post Mound Facies	Massive to thick bedded	Packstone to grainstone	Fusulinids, small forams, peloids, phylloid fragments	Shallow subtidal; deposition in depressions formed by phylloid mound accumulation.
Non-Skeletal Cap Facies	Massive	Wackdstone to framestone	Forams, whole *Chaetetes* heads	Shallow subtidal, well lit, high energy

Table 1. Summary of Lower Ismay facies.

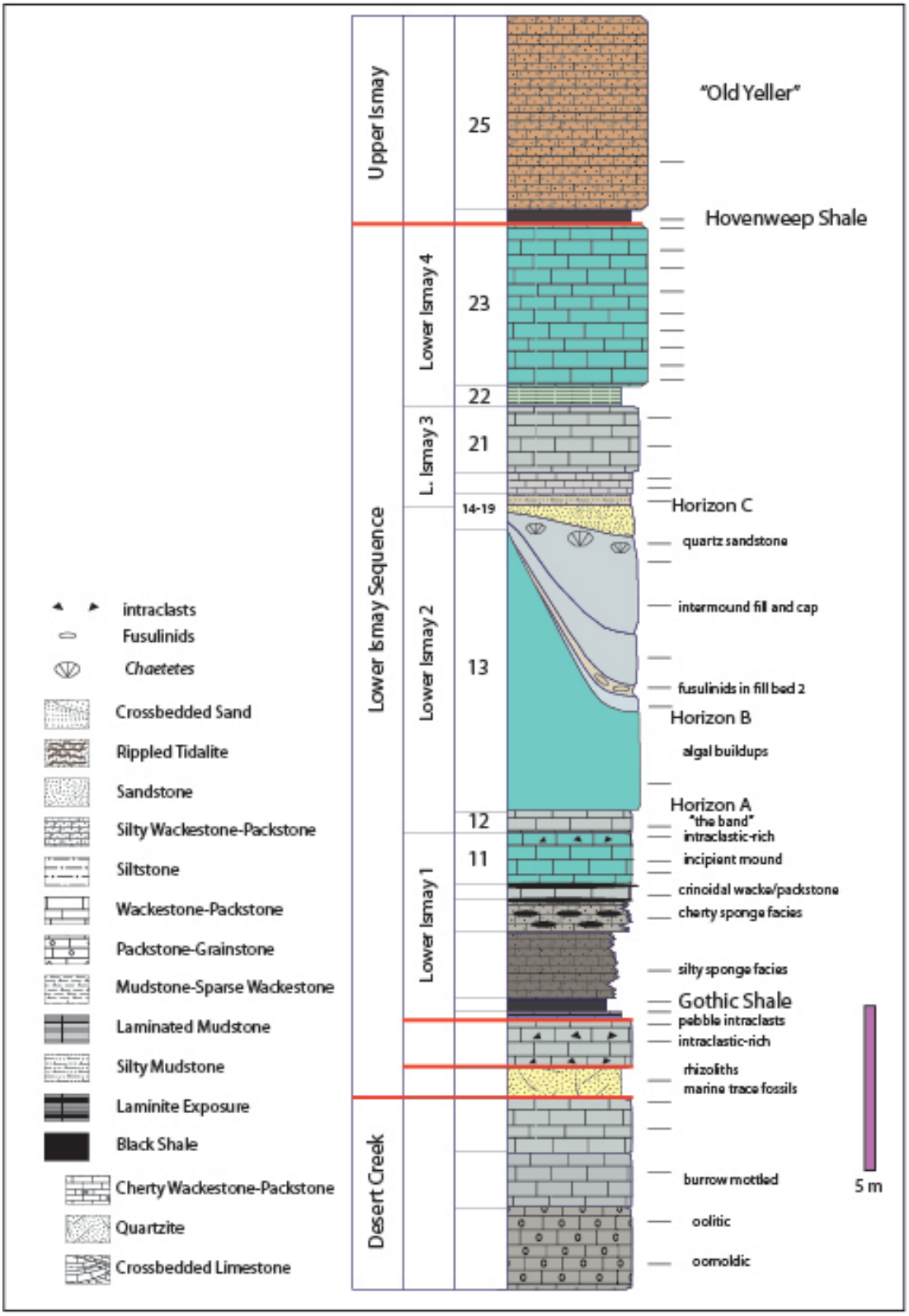

Figure 4. Lithostratigraphy and sequence stratigraphy of the Lower Ismay sequence and adjacent portions of the Upper Desert Creek and Upper Ismay sequences at Eight Foot Rapids.

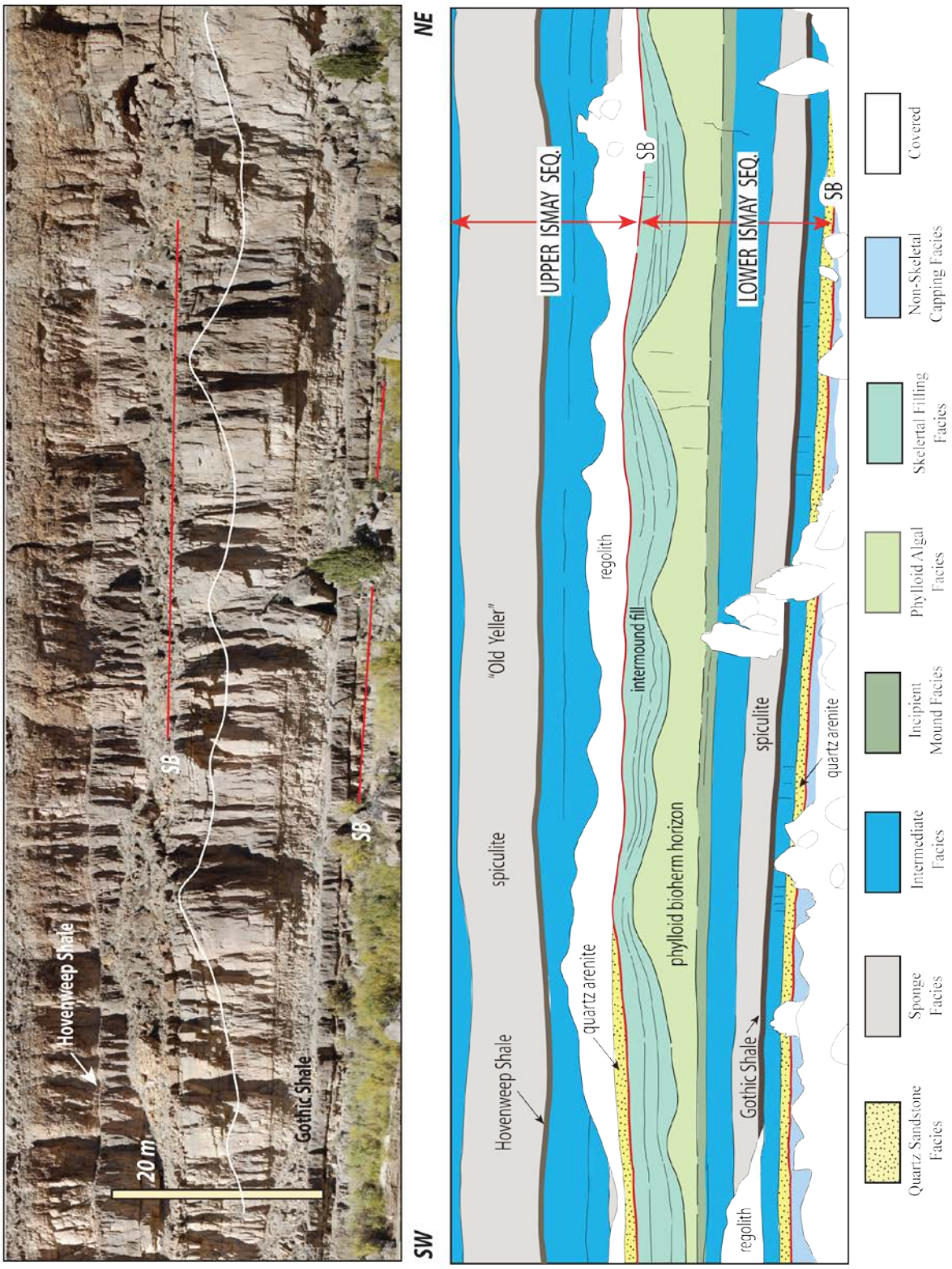

Figure 5. Outcrop character and facies composition of the Lower Ismay sequence and lower part of the Upper Ismay sequence in the vicinity of Eight Foot Rapids.

The Late Pennsylvanian section exposed at Eight Foot Rapid consists of numerous related facies of interest, varying from thin and laterally persistent carbonate strata, to lowstand clastic fills. The upper part of the section shows a distinct trend towards a less exclusively marine setting. The overall features, as noted by Pray and Wray (1964), suggest near-constant accumulation of sediments by the local carbonate factory, barring the erratic variations caused by local sequence stratigraphic processes.

In outcrop, the mounds of *Ivanovia* (Khvorova, 1946) are identifiable as gently undulatory "waves" with wavelengths approaching one-hundred to two-hundred feet. They range in thickness from 7m in the troughs to 14m at the crests. Underlying the bioherms is a transgressive mud-rich to mud-lean facies containing mostly heterozoan fauna but some photozoan as well. These facies include the noted Gothic Shale, the source rock for the Aneth Field.

Stevenson and Baars (1986) suggest that in the basin, extensional faulting and rapid basin subsidence began to magnify in Desmoinesian time, adding basinal evaporites and their shelf equivalent, to the Desmoinesian section of the Paradox Formation. Overlying the bioherms are intermound fills, deposited as accommodation space filled while sea level fell. This area shows a high diversity in heterozoan and photozoan flora and fauna, consistent with the shallowing of the Paradox seaway.

Ten percent of the hydrocarbons stored in the Aneth platform are localized in the lower Ismay sequence, with the remaining 90% residing in the lower and upper Desert Creek (Weber et al., 1995). Specifically for the purposes of this thesis, we'll be looking at the Lower Ismay, the portion of the Paradox Formation containing the phylloid algal mounds, although the lower Desert Creek underlying the Ismay contains the features as well.

The phylloid algal mounds develop from laterally extensive tidal-flat dolostones which hold a majority of their porosity as intercrystalline and moldic porosity. The moldic porosity accounts for the high storage capacity of the Aneth field, but the nature of the carbonates results in low permeability and subsequently difficult extraction.

Much of the regional architecture of both the phylloid algal mounds and the sequence framework were the focus of a study by Grammer et al. (1996). The undecided question currently is: are the phylloid mounds biological/diagenetic in genesis or are they the product of current alteration? Figure 3 shows these two dominant theories, the top being one of *in situ* growth, and bottom: hydrodynamic accumulation (Samankassou and West, 2003).

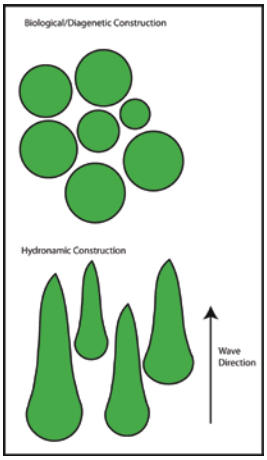

Figure 6: Two competing theories for mound formation.

Grammer and Ritter (2009) concluded some mounds were deposited "...in an environment more closely associated with strong currents" rather than the prevailing belief of *in situ* development advocated by Pray and Wray (1963).

Pray and Wray created the definitive stratigraphic study of the region, and interpreted the algal mound's sinusoidal surface as a time surface. This also demonstrated the algal mounds formed through, "…the lateral coalescing of more abrupt individual algal build-ups that formed by essentially *in-situ* clastic accumulation of algal fragments within a relatively turbulent marine environment." The morphology and spacing of these mounds is critical to testing this hypothesis.

DATA AND SURFACE MODELING

Analysis of the LIDAR data consisted of utilizing the programs AutoCAD and VirtuSurv to specifically extract data following three specific layers, hereby labeled as polylines A, B, and C (Figure 7).

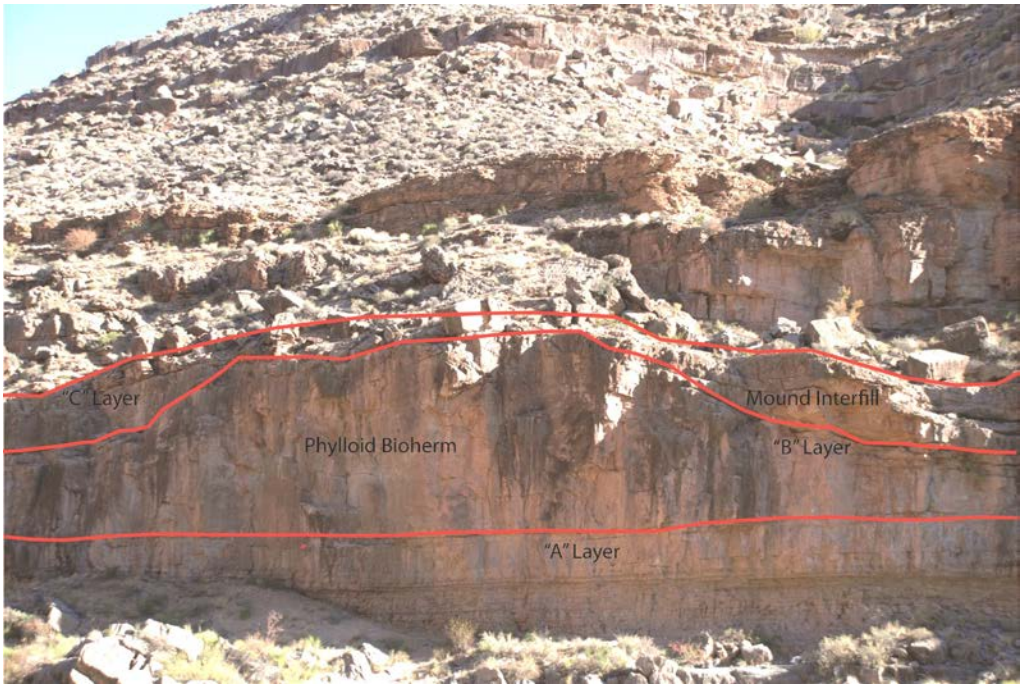

Figure 7. Outcrop showing stratigraphic position of surfaces A, B, and C. As is the lowest surface, C the highest.

Layer B is the most important layer of interest, mapping the morphology and shape of the algal mound surface. Surfaces A, and C act as both controls and additional support in mapping the precise dimensions of surface B.

Total Station data were used to fill in gaps in the LIDAR data that resulted from field logistics and the inaccessibility of certain stretches of the river. Combined, these data provide a complete wireframe that is loyal to the real-world dimensions of the outcrops along the canyon walls (Figure 8).

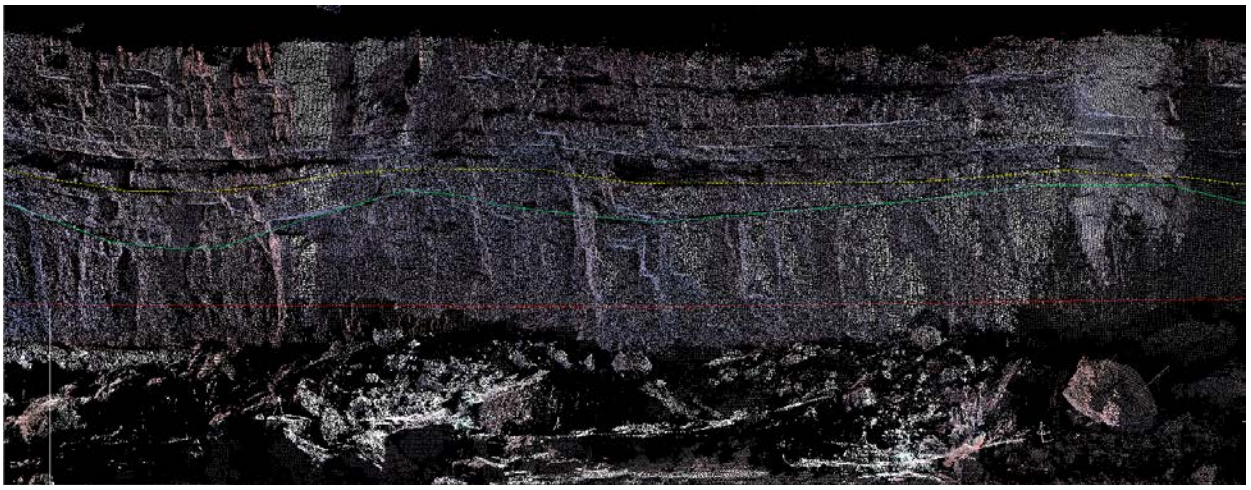

Figure 8. Specific surfaces mapped against LIDAR data of the canyon wall. Red line = surface A (base of algal mound bed), green line = top of algal mound interval, yellow line = sequence boundary between Lower and Upper Ismay sequences.

Figure 9 shows the data points collected from each of the three target layers. The bottom line (red) represents the base of the algal mounds. The middle line (green), more sinusoidal than the others, represents the algal surface, and the top line represents the boundary between the Lower and Upper Ismay sequences.

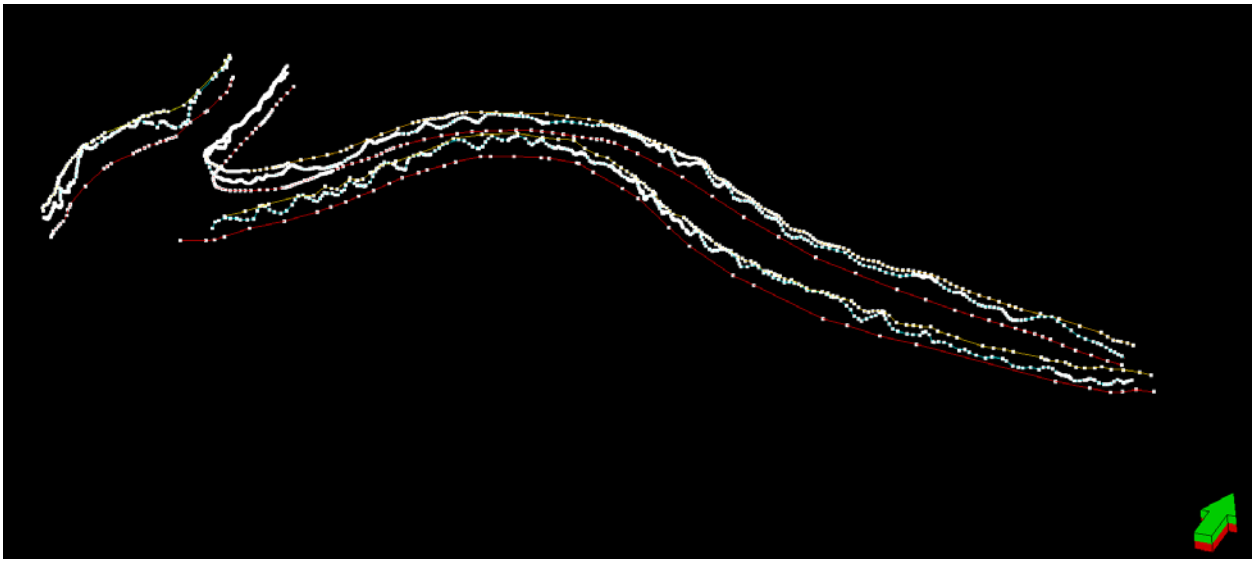

Figure 9: Isolated points of the relevant area mapped in 3d. Vertically exaggerated by four times.

The swaths were then isolated and put into a flattened plane in order to analyze the different mound structures (Figure 10). From there, the base level for the mounds is set at a constant height of 1280 m in order to remove effects of Laramide folding and to analyze the height of the mounds above the base (Figure 11).

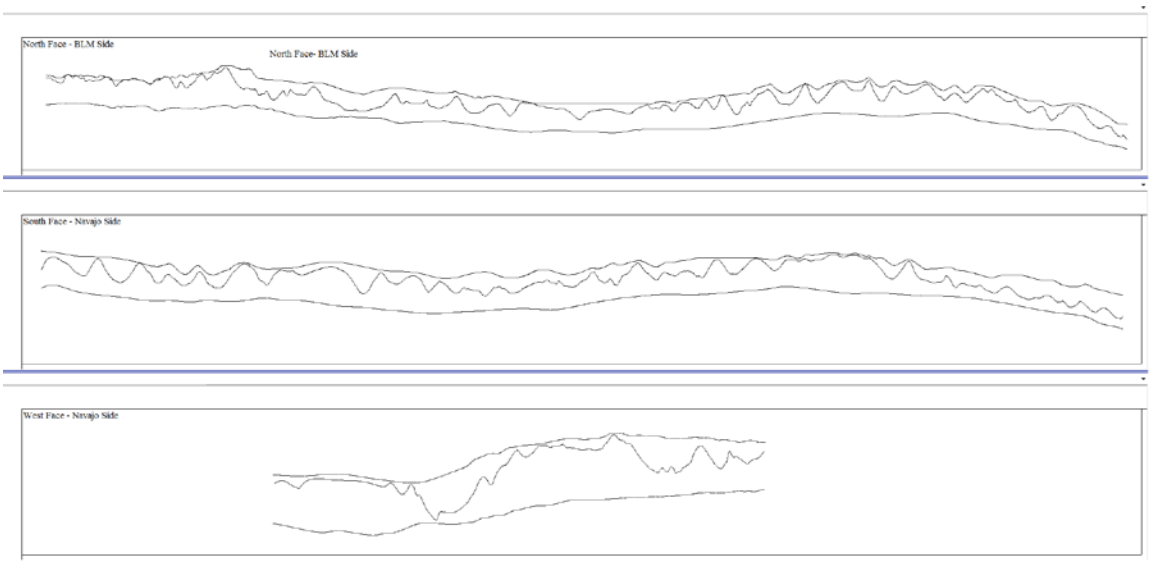

Figure 10. Three pans of the canyon walls along the San Juan River. All pans are vertically exaggerated four times and are flattened into a 2d plane.

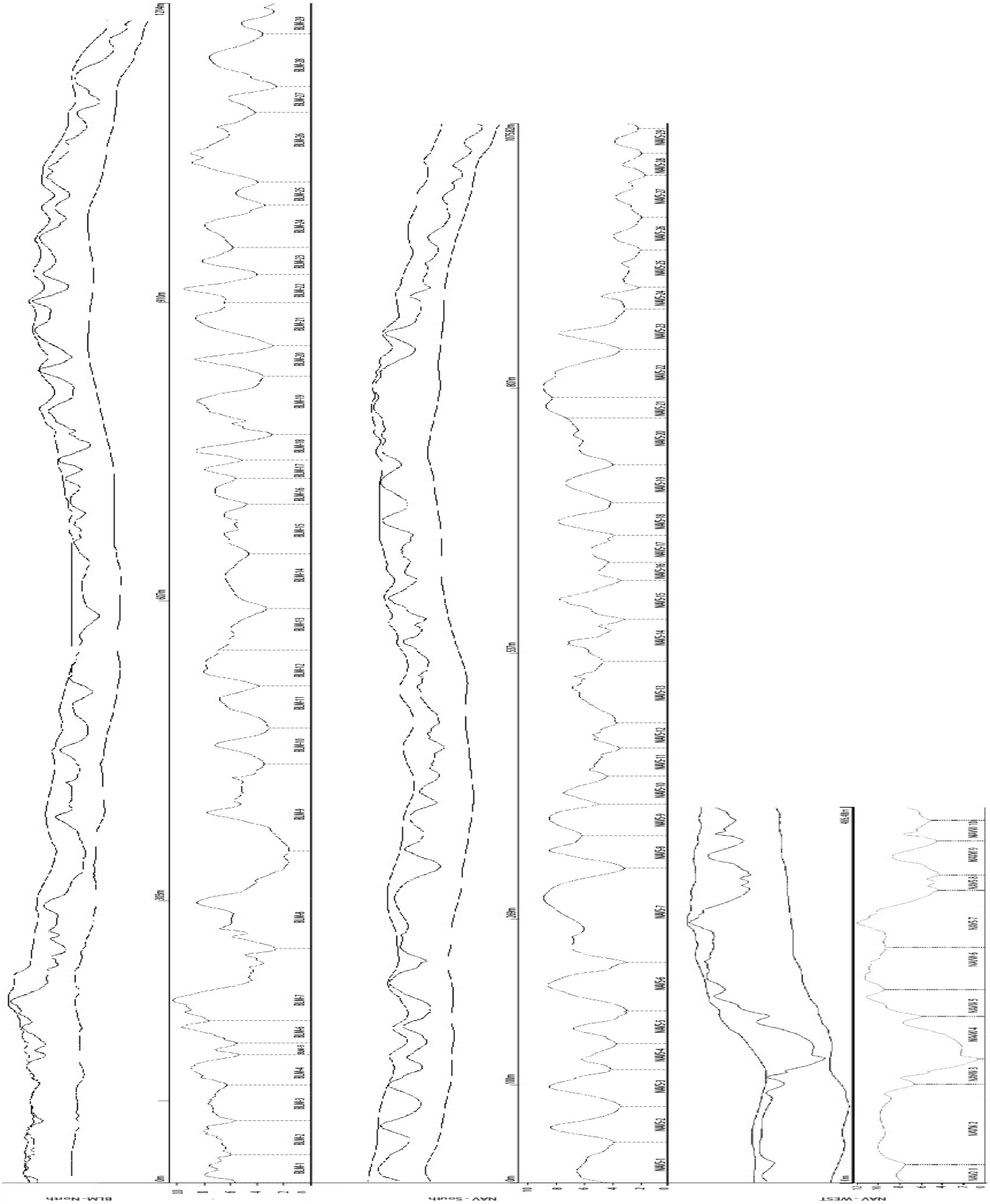

Figure 11. Three previous pans where the baseline is set at a constant value in order to measure the height above the base of the mounds, in order to make the field similar to the topography at the time of deposition. Mounds are

numbered and named where BLM refers to the northern Bureau of Land Management side of the river, and NAVW and NAVS refers to the west and southern pans of the Navajo side of the river. All data is vertically exaggerated.

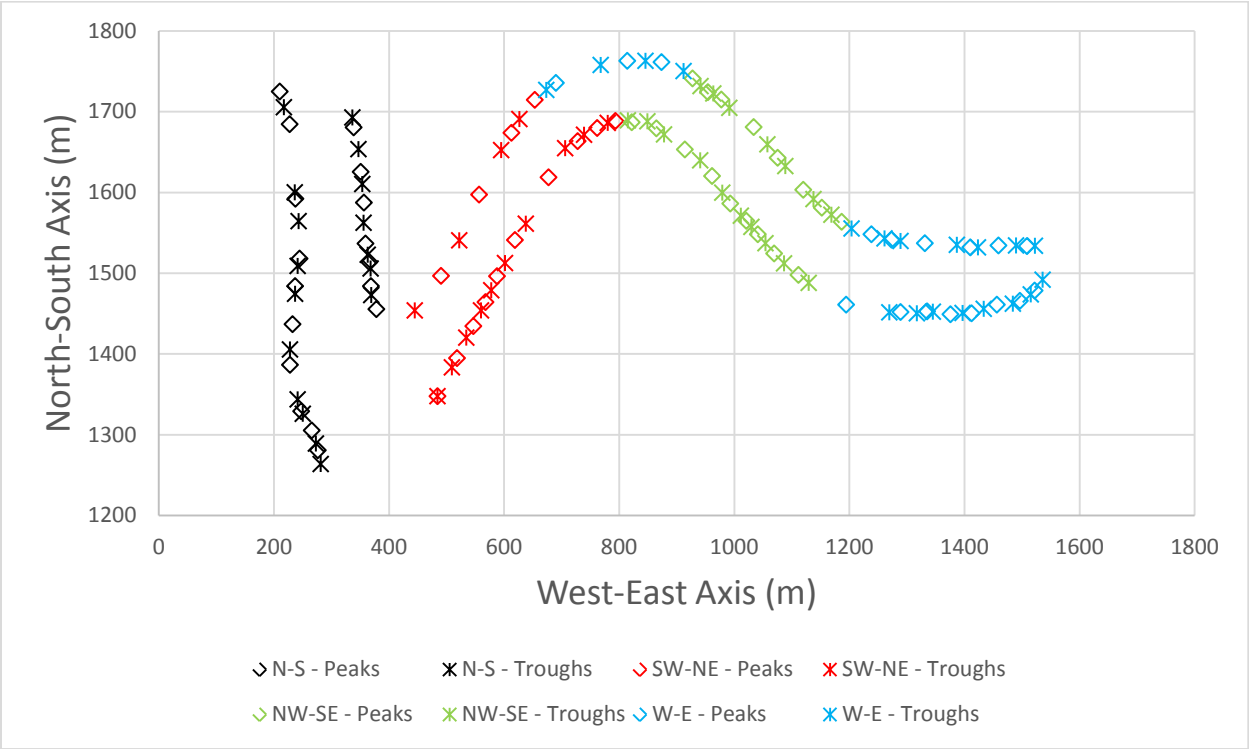

Figure 12. Regional overview of peaks and troughs along the San Juan River.

Figure 12 shows the pans subdivided into azimuth specific groups. This was done in order to preserve the azimuth of the data so that the following statistical analyses are as well preserved and isolated into these specific groups.

The points comprising polylines derived from layers A, B, and C were subsequently imported into Microsoft Excel and the points marking the individual peaks and troughs of the algal fields were extracted. Table 2 shows the number of these troughs and peaks, and Figure 12 shows those troughs and peaks in geographic terms.

	Peaks	Troughs
Northern Pan	28	29
Southern Pan	37	38
North-South	17	17
Southwest-Northeast	14	14
Northwest-Southeast	17	17
West-East	17	19

Table 2. Table displaying the number of peaks and troughs located along the Eight Foot rapid section of the San Juan River. North-South, Southwest-Northeast, Northwest-Southeast, and West-East categories are merged from

both the South and Northern Pan pointset, combining points with similar azimuths.

These points were subjected to statistical analysis in order to identify trends within the data that would reveal depositional history and geomorphology in the subsurface. It is important to note the river's shape plays a role in properly understanding the subsurface as it provides glimpses into an almost 360° pan of the algal surface, something which would be hard to accomplish were we merely examining two sides of a straight river.

The main parameters collected and studied are azimuth of trough outrops, the horizontal distance between troughs, the height of algal peaks above the base layer (referred to here as "depth"), and the spatial x and y coordinates (corresponding to the cardinal directions).

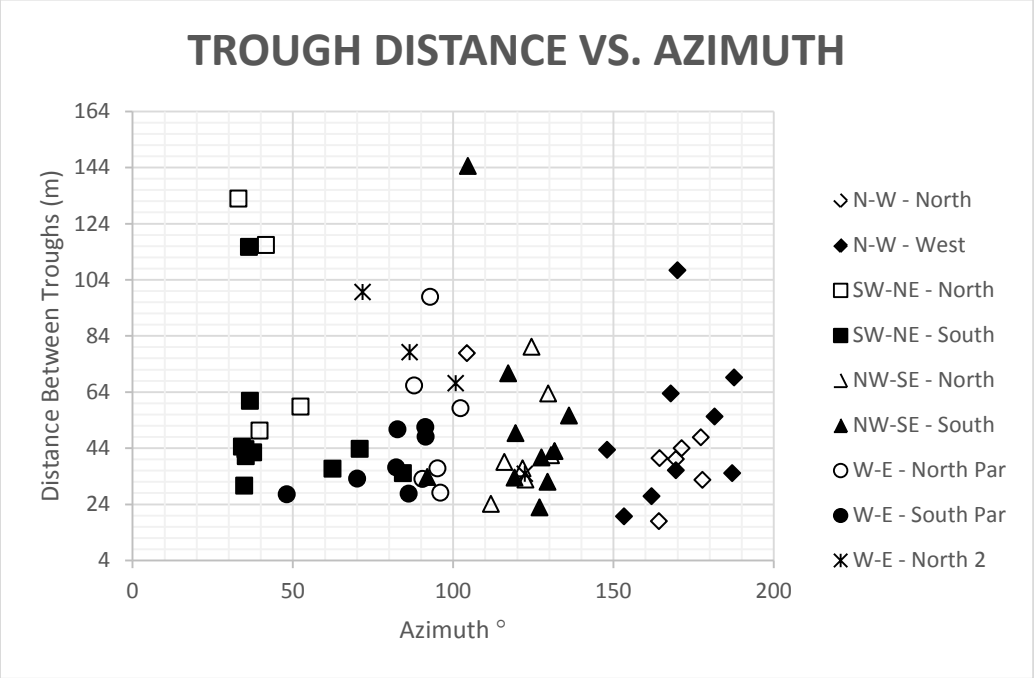

Figure 13. Graphic showing trough to trough distance versus the azimuth of the trough.

Given the supposition that there is a linear trend present in the subsurface, there would therefore be evidence displayed in the rock record itself. Namely that if there is a preferred direction and elogation of the mounds then the length of the mound structures would be weighted accordingly. Elogated mounds would be shown as having greater wavelengths than the shortened mounds. Figure 13 displays this in graphical form. Again, this data has been diveded up into different tracts along the walls, in order to differentiate data following the trend of the canyon wall.

Were the hypothesis of mound lengthening true, then there would be a linear trend present in the data, with high Y axis values (mound wavelength) marking the elongated axis and lower values indicating the shortened wavelength. Data clustering is important as it indicates that all the samples of a specific azimuth all share similar trough distance. The less clustering means there is less of a trend. At first glance, an argument could be made for data clustering, but given the low number of reported values and an absence of any true trend, the null hypothesis of no elongation must be accepted.

	Total	North	N-S	SW-NE	W-E	NW-SE	W-E	South	SW-NE	NW-SE	W-E	West
RSQ	0.11		0.4993	0.6125	0.0723	0.3481	0.1018		0.0284	0.0849	0.3681	0.2190

Table 3. R^2 values for the parameters of Figure 12

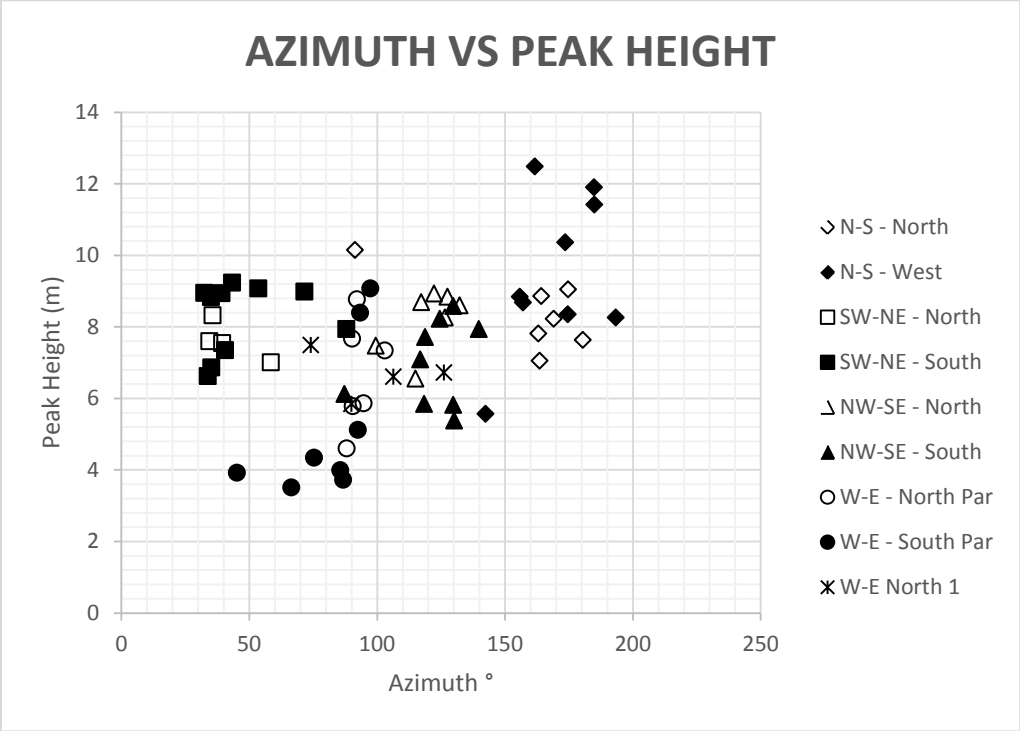

Figure 14. Graphic charting trough-to-trough Azimuth against peak height.

Figure 14 goes further and checks if there is any relationship between the azimuth and the height of the mounds. Assuming there is a preferential elogation, one would expect that azimuths running strike parallel would tend towards following the highest part of the mound crest, one those running dip parallel might simply be cutting alongside the flanks of the mound. As before, there does seem to be preferential clustering, but the data is still too loose and unrelated to allow for the hypothesis of elongation, so the null hypothesis must be accepted.

	Total	North	N-S	SW-NE	W-E	NW-SE	W-E	South	SW-NE	NW-SE	W-E	West
RSQ	0.045		0.600	0.394	0.988	0.310	0.017		0.081	0.121	0.418	0.103

Table 4. R^2 values for the parameters of Fig 13.

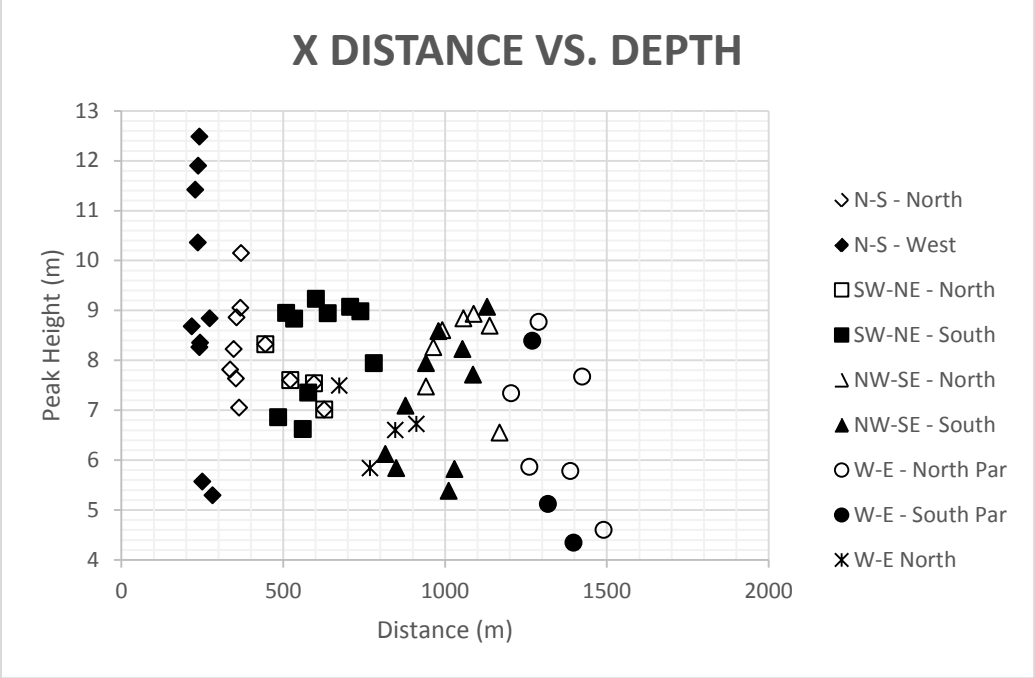

Figure 15. Graphic showing spatial distance from west to east against depth.

Figure 15 displays spatial distance from west to east against depth.Since the hypothesis of elogation does not appear to be conclusive, instead we'll examine any inherant trends within the mounds. Examining the height of the mounds plotted against geographical location will show if there is any inherant changes as one moves basinward or landward. While the data does not appear any conclusive, the addition of both an x and y axis as well as the z axis of mound height lets us get a better view of any sort of trends.

	Total	**North**	**N-S**	**SW-NE**	**W-E**	**NW-SE**	**W-E**	**South**	**SW-NE**	**NW-SE**	**W-E**	**West**
RSQ	0.380		0.241	0.891	0.129	0.023	0.448		0.11	0.252	0.668	0.297

Table 5. R^2 values for the parameters of Figure 14.

Figure 17 shows those directions with West-East directions being defined as vXPeaks and our North-South directons being defined as vYPeaks.

Looking back at Figure 12 shows this XYZ chart, giving us a better view of the data. Figure 17 is then fitted with a regression plane to map the points in all three dimensions. There is an obvious trend noticable in the data, namely that the farther west one goes, the higher the mounds tend to be. There is a slight North-South trend as well, but it is slight enough that one cannot make a definivite argument as to the statistical significance of the direction. This can be explained as the mounds all developing at a specific water depth. The changes in size occur as sea level fluctuates higher, leaving the more basinward mounds in deeper water where mound generation is not ideal.

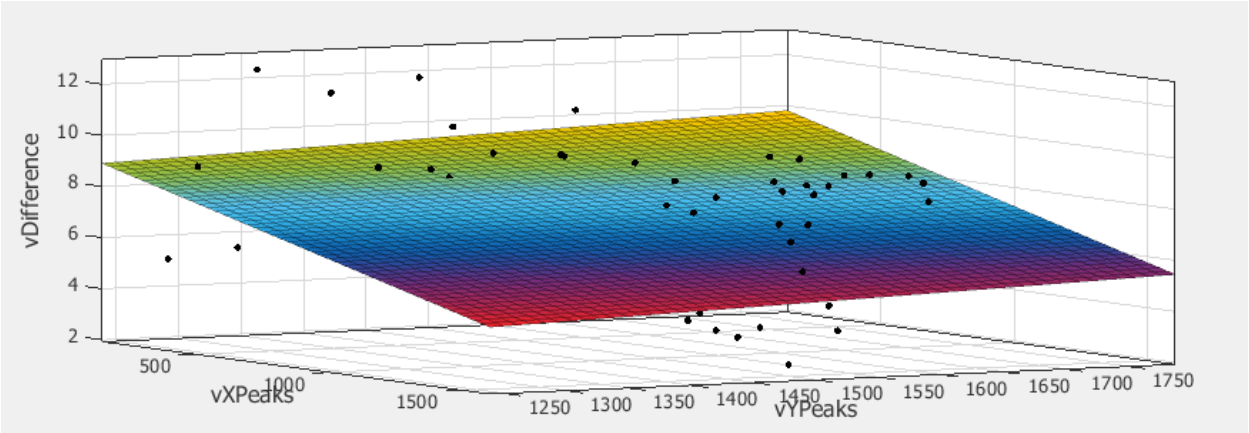

Figure 17. View of plane fit to peak height data. The same as figure 15 above, only rotated to show X, Y, and Z axes. X and Y-axes still use the same values. An obvious trend, specifically along the vXPeaks axis is notable. The plane shows an increase as the vXPeaks value decreses (the farther west one travels) then the vDifference increases (mound height increases). This shows there is likely a pattern between the West-East direction and mound height.

SHAPE FITTING

In order to better understand the mound systems, an interpretation of the subsurface must be made using the examined statistics generated from the previous data. Figure 18 shows a sample grouping of existing mounds modified so that their data will fit into a Gaussian curve, which for our purposes will approximate the mound shape after deposition but before burial. Force fitting them to a Gaussian curve will make the mounds look equidimensional, but given the stochastic modeling to follow, perfect recreations aren't necessary. Only a standard set of parameters are needed to typify the mounds. Due to the east-west trend of mounds, numerous theoretical mounds will need to be mapped in order to more fully recreate the ancient shoreline complex.

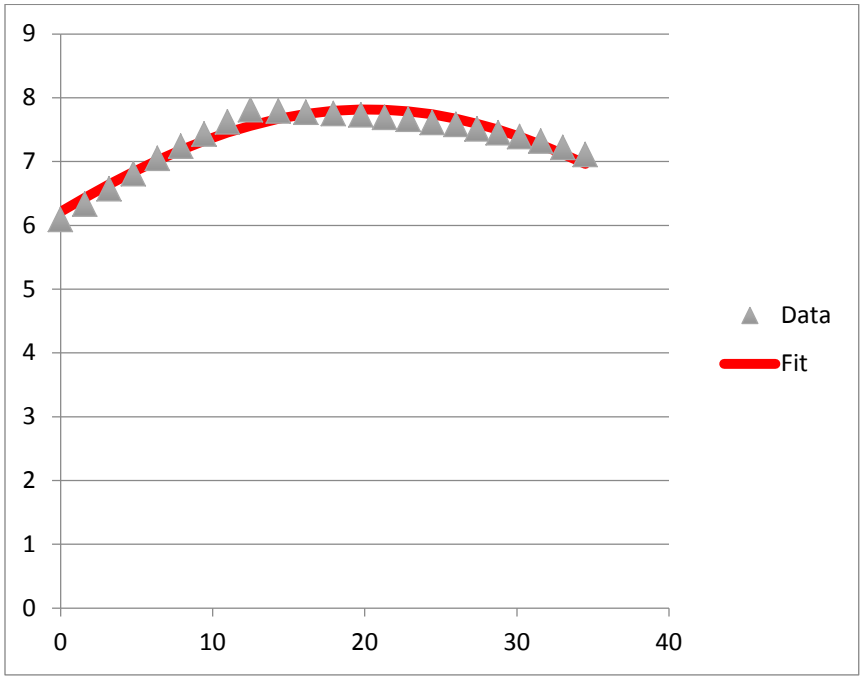

Figure 18. Real mound modeled against data fit to gaussian curves.

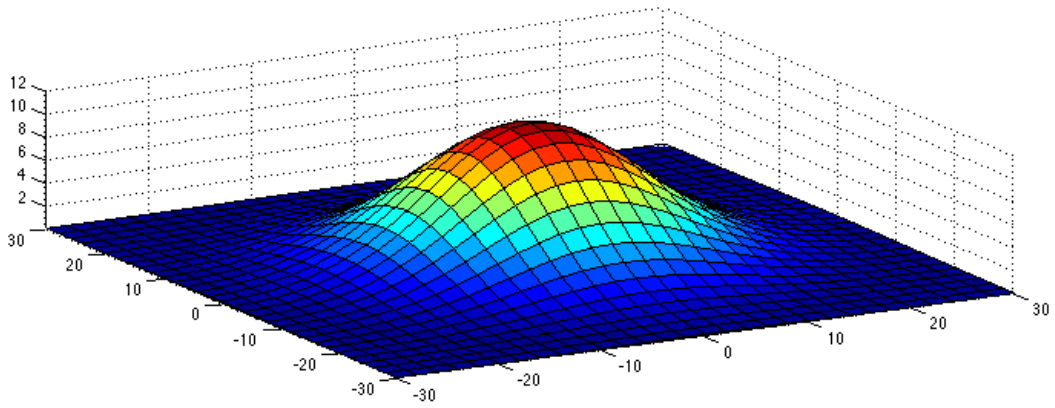

Figure 19: Theoretical algal mound using predicted parameters.

Figure 19 shows the modeled mound using some sample parameters and further research will involve replicating this mound structure in order to fully recreate the field at the time of deposition and decide a best fit model for the data as a whole.

As mentioned earlier in the paper, knowledge of the full morphology could be unnecessary if the entire system is proven to be interconnected. Further studies will therefore be necessary to include a more in-depth analysis of the facies within the mounds themselves in order to more properly understand flow patterns and communication between mound systems.

CONCLUSIONS

This study provides compelling evidence towards the interpretation of the phylloid algal mounds and their methods of formation. The ideas of hydrodynamic processes constituting a major role is unlikely due to the statistics analyzing the mound azimuths and shapes which seem to be independent of the position of the algal mounds when related to the ancient shoreline.

Our approach to this thesis first involved utilization of both LIDAR and total station data points in order to generate a workable 3d model of the Eight-Foot Rapids environment. From there, the steps to data analysis as well as what can be further expanded on were as follows:

1. Export data into usable format
2. Generate statistics (standard deviation, azimuth, etc)
3. Model statistics against each other, looking for correlations

4. Create Gaussian curves fitted to the data
5. Using any correlations discovered, combine that with Gaussian curve statistics to generate idealized model sets
6. Generate randomized algal fields to reconstruct the ancient shoreline.

The essence of the study looks to understand the morphology of the mound shapes, but only touches at the bigger picture of whether mound shape is of vital importance from the petroleum generation standpoint. Whether or not the mounds are separate from each other or are continuous adds further debate to the point. If there is continuity then gravity drainage could play a big impact because if a single mound is penetrated too high in the mound, then the resulting depletion could leave bypassed pay in the apex of the connecting mounds.

Thus far, our findings have indicated there is a likely correlation between the geographic location of a mound and its height. This lends itself towards the interpretation of the mounds as isolated formations generated at the same water depths but varying depending on sea level fluctuation. Basinward mounds are therefore smaller as there is less time for accumulation due to being too far below the ideal zone for mound formation. Our findings thusly reject the hypothesis of mound formation as a function of hydrodynamic processes such as tidal forces or longshore currents. Further studies will be performed in order to more fully examine and model the subsurface in order to more fully understand the manner of formation during the time of deposition.

REFERENCES

Babcock, J.A., 1977, Calcareous algae, organic boundstones, and the genesis of the upper Capitan Limestone (Permian, Guadalupian) , Guadalupe Mountains, west Texas and New Mexico. In, Hileman, M.E. and Mazzullo, S.J., (eds.), Upper Guadalupian facies, Permian reef complex, Guadalupe Mountains, New Mexico and west Texas. Society of Economic Paleontologists and Mineralogists, Permian Basin Section, Special Publication 77/6, p. 3-44.

Ball, S.M., Pollard, W. D., and Roberts, J. W., 1977, Importance of phylloid algae in development of depositional topography—reality or myth? In, Frost, S.H, Weiss, .P., Saunders, J.B., (eds), Reefs and related carbonates—ecology and sedimentology. American Association of Petroleum Geologists Studies in Geology no. 5, p. 239-260.

Brinton, L., 1986, Deposition and diagenesis of middle Pennsylvanian (Desmoinesian) phylloid algal banks, Paradox Formation, Ismay Zone, Ismay field and San Juan canyon, Paradox Basin, Utah and Colorado. Golden, Colorado School of Mines, unpublished Ph.D. thesis, 315 pp.

Chidsey, T.C., Jr., Brinton, L., Eby, D.E., and Hartmann, K., 1996, Carbonate-mound reservoirs in the Paradox Formation: an outcrop analogue along the San Juan River, southeastern Utah. In: Huffman, A.C., Jr., Lund, W.R., and Godwin, L.H. (eds.), Geology and Resources of the Paradox Basin, Utah Geological Association Guidebook 25, p. 139-150.

Choquette, P.W., and Traut, J.D., 1963, Pennsylvanian carbonate reservoirs, Ismay field, Utah and Colorado. In Bass, R.O. (ed.), Shelf carbonates of the Paradox Basin: Four Corners Geological Society 4th Field Conference Guidebook, pp. 157-184.

Cross, T.A., and Klostermann, M.J., 1981a, Autecology and development of a stromatoltic-bound phylloid algal bioherm, Laborcita Formaton (lower Permian), Sacramento Mountains, New Mexico, USA. In: Monty, C. (ed.), Phanerozoic Stromatolites. Springer-Verlag, Berlin, p. 45-59.

Cross, T.A., and Klostermann, M.J., 1981b, Primary submarine cements and neomorphic spar in a stromatolic-bound phylloid algal bioherm, Laborcita Formatio (Wolfcampian), Sacramento Mountains, New Mexico, USA. In: Monty, C. (ed.), Phanerozoic Stromatolites. Springer-Verlag, Berlin, p. 60-73.

Elias, G.K., 1963, Habitat of Pennsylvanian algal bioherms, Four Corners area. In Bass, R.O. (ed.), Shelf carbonates of the Paradox Basin: Four Corners Geological Society 4th Field Conference Guidebook, p. 185-203..

Fagerstrom, J.A., 1987, The Evolution of Reef Communities. New York, John Wiley and Sons, 592 p.

Forsythe,G.T.W., 2003, A new synthesis of Permo-Carboniferous phylloid algal reef ecology. In Permo-Carboniferous Carbonate Platforms and Reefs. SEPM Special Publication No. 78 and AAPG Memoir 83

Gianniny, Gary L. and Simo, J.A.T., 1996, Implications of unfilled accomodation space for sequence stratigraphy on mixed carbonate-siliciclastic platforms; An example from the lower Desmoinesian (Middle Pennsylvanian), southwestern Paradox Basin, Utah, in Longman, M.W.and M.D.Sonnenfeld, eds., Paleozoic systems of theRocky Mountain region. Society for Sedimentary Geology, Rocky Mountain Section, p. 213-234.

Gianniny, G.L., and Miskell-Gerhardt, K.J., 2009, Progradational mixed siliciclastic/carbonate sequence sets on the tectonicallyactive eastern margin of the Pennsylvanian Paradox Basin, southwestern Colorado, in Houston et al (eds.), 2009, The Paradox Basin

Revisited – New Developments in Petroleum Systems and Basin Analysis: RMAG Special Publication, p. 310-380.
Giles, K.A., Soreghan, G.S., 1999, Altitudes of Late Pennsylvanian glacioeustasy: Geology, v. 27, no. 3, p. 255-258.
Goldhammer, R.K., Oswald, E.J., and Dunn, P.A., 1991, The hierarchy of stratigraphic forcing: An example from Middle Pennsylvanian shelf carbonates of the Paradox Basin. In Franseen, E. K. (ed.), Sedimentary Modelling – Computer simulations and methods for improved parameter definition. Kansas Geological Survey Bulletin 233, p. 361-413.
Grammar, G.M., Eberli, G.P., Van Buchem, F.S.P., Stevenson, G.M., and Homewood, P., 1996, Application of high-resolution sequence stratigraphy to evaluate lateral variability in outcrop and subsurface-Desert Creek and Ismay intervals, Paradox Basin. In: Longman, M.W., and Sonnenfeld, M.D. (eds.), Paleozoic systems of the Rocky Mountain region. Rocky Mountain section SEPM (Society for Sedimentary Geology), p. 235-266.
Grammer, G.M., Ritter, A.L., 2009, Phylloid algal mounds in the Paradox Basin, southwestern U.S.A. - an alternative to the *in situ* constructional growth model? In Swart, P.K., Eberli, G.P., and McKenzie, J.A., (eds.), Perspectives in Carbonate Geology, International Association of Sedimentologists, Special Publication, no. 4, p. 239-354.
Heckel, P.H., and Cocke, J.M., 1969, Phylloid algal-mound complexes in outcropping Upper Pennsylvanian rocks of Mid-Continent. American Association of Petroleum Geologists, Bulletin v. 53, p. 1058-1074.
Hite, R. J., 1960, Stratigraphy of the saline facies of theParadox Member of the Hermosa Formation ofsoutheastern Utah and southwestern Colorado: FourCorners Geological Association, 3rd Annual Field Conference Guidebook, p. 86-89.
Khvorova, I.V., 1946, On a new genus of algae from the Middle Carboniferous deposits of the Moscow Basin. Compte Rendus de l'Academie des Sciences de l'URSS v. 23, p. 737-739.
Konishi, K., and Wray, J.L., 1961, *Eugonophyllum,* a new Pennsylvanian and Permian algal genus. Journal of Paleontology, v. 35, p. 659-666.
Mazzullo, S.J., and Cys, J.M., 1979, Marine aragonite sea-floor growths and cements in Permian phylloid algal mounds, Sacramento Mountains, New Mexico. Journal of Sedimentary Petrology, v. 49, p. 917-936.
Pray, L.C. and Wray, J.L., (1963) Porous algal facies (Pennsylvanian) Honaker Trail, San Juan Canyon, Utah. In: Bass, R.O. (ed.), Shelf Carbonates of the Paradox Basin: Four Corners Geological Society 4th Field Conference Guidebook, pp. 204-234.
Rasmussen, L., and Rasmussen, D.L., 2009, Burial history analysis of the Pennsylvanian petroleum system in the deep Paradox Basin Fold and Fault Belt, Colorado and Utah. In Houston et al., The Paradox Basin Revisited – New Developments in Petroleum Systems and Basin Analysis: RMAG Special Publication, p. 24-94.
Ritter, S.M., Barrick, J.E., and Skinner, M.R., 2002, Conodont sequence biostratigraphy of the Hermosa Group (Pennsylvanian) at Honaker Trail, Paradox Basinm Utah. Journal of Paleontology, v. 76, 495-517.
Samankassou, E., and West, R.R., 2002, Construction versus accumulation in phylloid algal mounds: an example of small constructed mounds in the Pennsylvanian of Kansas USA. Palaeogeography, Palaeoclimatology, and Palaeoecology, v. 185 p. 379-389.
Samankassou, E., and West, R.R., 2003, Constructional and accumulational modes of fabrics in selected Pennsylvanian algal-dominated buildups in eastern Kansas, Midcontinent,

U.S.A. In Ahr, W.M., Harris, P.M., Morgan, W.A., and Somerville, I.D. (eds.) Permo-Carboniferous platforms and reefs, SEPM/AAPG Special Publication 78, p. 219-237.

Stevenson, G.M., and Baars, D.L., 1986, The Paradox—A pull-apart basin of Pennsylvanian age, in Peterson, J.A., ed., Paleotectonics and sedimentation: American Association of Petroleum Geologists Memoir 41, p. 513–539.

Toomey, D.F., and Babcock, J.A., 1983, Precambrian and Paleozoic algal carbonates, west Texas-southern New Mexico. Colorado School of Mines, Golden, Professional Contributions no. 11, 345 pp.

Weber, L.J., Sarg, J.F., and Wright, F.M., 1995, Sequence stratigraphy and reservoir delineation of the Middle Pennsylvanian (Desmoinesian), Paradox Basin and Aneth field, Milankovitch sea-level changes and reservoirs on carbonate platforms in greenhouse and ice-house worlds. SEPM (Society for Sedimentary Geology) Short Course no. 35, p. 1-81.

Willis, G.C., Doelling, H.H., Weber, L.J., and Wright, F.M., 1996, Second day road and river log. In Huffman, A.C., Jr., Lund, W.R., and Godwin, L.H. (eds.), Geology and Resources of the Paradox Basin, Utah Geological Association Guidebook 25, p. 429-460.

APPENDICES

See CD

Contents

Stats 1. Contains statistical formulas and graphs showing mound curves fitted to normalized curves.

Stats 2. Contains standard statistical parameters categorized by mounds. Includes standard deviation, etc.

Stats 3. Contains parameters seen in Stats 2. Main calculations document.

Stats 4. Contains statistical calculations used to create azimuth vs. trough, etc graphics.

Stats 5. Contains peaks and troughs calculations. Base pages from other stats documents.

XYZ Data – raw data files from LIDAR survey.